optica

Generation of intense supercontinuum in condensed media

CHIH-HSUAN LU,[1] YU-JUNG TSOU,[1] HONG-YU CHEN,[1] BO-HAN CHEN,[1] YU-CHEN CHENG,[2] SHANG-DA YANG,[1] MING-CHANG CHEN,[1] CHIA-CHEN HSU,[3] AND A. H. KUNG[1,2,*]

[1]Institute of Photonics Technologies, National Tsing Hua University, Hsinchu 30013, Taiwan

[2]Institute of Atomic and Molecular Sciences, Academia Sinica, Taipei 10617, Taiwan

[3]Department of Physics, National Chung Cheng University, Chiayi 62102, Taiwan

*Corresponding author: akung@pub.iams.sinica.edu.tw

Received 2 September 2014; revised 16 October 2014; accepted 29 October 2014 (Doc. ID 222144); published 10 December 2014

Destructive nonlinear processes have limited the useful input power to a few megawatts for supercontinuum generation in bulk material. Consequently, reliable high-power, high-pulse-energy supercontinuum in condensed media has not been realized. Here, we describe an intense femtosecond supercontinuum generated in a solid medium with pulse energy and mode quality that approach those generated in the gas phase while preserving the advantages of a condensed medium of being compact, simple to operate, and highly reproducible. This is achieved by strategically placing several thin solid plates at or near the focused waist of a high-power laser pulse. The thickness of each plate is such that the optical pulse exits the plate before undesirable effects begin to take hold of the pulse. With this approach, we have obtained pulses that have an octave-spanning spectrum that covers from 450 to 980 nm at the −20 dB intensity level while converting as much as 54% of the input pulse energy to the continuum. The highest pulse energy obtained to date is 76 μJ, nearly two orders of magnitude greater than previously reported values. The transverse mode of the pulse has a M^2 of 1.25. Frequency-resolved optical grating and spectral interferometric measurements indicate that the pulse is phase coherent and could be compressed to a few femtoseconds. Furthermore, the multiple-plates approach is shown to be extremely flexible and versatile. It is applicable for a broad range of input powers and materials. The generated continuum is stable and robust. Thus, multiple-plate generated femtosecond continuum could be a promising new light source in ultrafast science and extreme nonlinear optics applications.

OCIS codes: (320.6629) Supercontinuum generation; (190.7110) Ultrafast nonlinear optics; (320.7100) Ultrafast measurements.

http://dx.doi.org/10.1364/OPTICA.1.000400

1. INTRODUCTION

Supercontinuum generation (SCG) is a universal process that takes place in gases, liquids, and solids [1]. A supercontinuum is characterized by an extremely broad pedestal that extends to the blue in the transmitted pulse spectrum. It is a broadly tunable ultrafast spectroscopic source of radiation that has important applications in attosecond science for the synthesis of subcycle pulses and for isolated pulse high harmonic generation [2–4]. SCG is also an important source in carrier–envelope phase stabilization [5,6], metrology [7], microscopy beyond the diffraction limit [8], and optical coherence tomography [9]. The dynamics of SCG are well studied and shown to be quite complicated [see, e.g., 10–12]. Detailed analyses have shown that the blue pedestal in SCG originates from the formation of an optical shock as a result of space-time focusing of the pulse. SCG is also associated with filament formation, which is a consequence of self-focusing and plasma formation due to multiphoton absorption and ionization.

The general picture in all the theory and experimental studies is that there is a threshold power which is just slightly higher (less than 2 times) than the critical power P_{cr} for self-focusing in the medium. Here, $P_{cr} = 3.77\lambda^2/(8\pi n_o n_2)$ where λ is the laser wavelength, n_o is the linear index of refraction, and n_2 is the nonlinear index of refraction of the medium. For gases, typical P_{cr} is in the 10 GW range, which is now readily obtainable from many near-IR femtosecond laser systems. The nonlinear index n_2 in condensed media is typically 1000 times larger than in gases, so that P_{cr} in condensed media is in the range of MWs [11–13].

SCG is further characterized by a sharp roll-off on the blue end of the spectrum. This is because when the input power P rises above the threshold power for SCG, multiphoton absorption and plasma formation begin to play a significant role. The peak intensity is clamped [14], prohibiting further spectral expansion. Furthermore modulational instability sets in, making way for multiple filamentation and pulse breakup and eventually optical breakdown and damage [10–17]. The transverse mode quality of the pulse is destroyed; light transmission drops severely. Although SCG in bulk can now cover from 450 to 4500 nm [18], it is still limited to input peak power of a few MW and the integrated pulse energy remains at the few μJ level. Reliable high power SCG in condensed media has not been realized.

Studies that carefully track the evolution of SCG and the collapse of the pulse show that spectral expansion precedes pulse splitting or optical breakdown [17,19]. This means there is a window in time and space where spectral expansion has progressed with the pulse remaining intact. If we limit the medium thickness, the laser pulse will have an expanded spectrum but will exit the medium before multiple filamentation and damage begin to occur. The exiting pulse will be chirped. Once outside the medium, nonlinear phase collected by the pulse while inside the medium will cause the pulse to refocus in space and recompress in time. The pulse could self-heal while propagating in air [20]. The pulse intensity may then be recovered. Hence, by placing additional thin plates downstream in the optical path, more rounds of spectral expansion may be repeated to yield a broad spectrum until multiphoton absorption, pulse chirp, and/or beam diffraction cause the pulse power and intensity to drop below the threshold for further spectral expansion.

Here, we describe the management of a solid medium for high-power femtosecond continuum generation. By strategically placing thin plates of fused silica at or near the waist of a high-power laser pulse, we have succeeded in generating a stable and intense ultrafast white light continuum. The generated octave-spanning spectrum covers from 450 to 980 nm at the −20 dB intensity level. As much as 54% of the input pulse energy is converted to the continuum. The transverse mode of the pulse has a M^2 of 1.25. FROG measurements and spectral interferometric measurements indicate that the pulse is chirped to about 300 fs, but it is phase coherent and could be compressed to a few femtoseconds. We show that this multiple-plates approach is functional for a broad range of input pulse energies, at least from 20 to 140 μJ in a 25 fs pulse. There have been numerous reports on SCG in fused silica (see [13,15–17] and references therein). This is the first time that the continuum pulse energy could have the possibility of being scaled to reach that obtained in a gas medium [21] with good mode quality while preserving the advantages of compactness, easy alignment, and simple operation of a condensed medium.

2. EXPERIMENT

Transform-limited 25 fs pulses from a 1 kHz chirp-pulse-amplified Ti:sapphire laser were focused to an intensity of 1.9×10^{13} W/cm^2, calculated at normal incidence and without taking self-focusing in air into account. The corresponding fluence of 0.47 J/cm^2 is below the dielectric damage threshold of 1–2 J/cm^2 for femtosecond pulses in fused silica [22,23]. The pulse-to-pulse energy fluctuation was approximately ±0.4% (one standard deviation), and the transverse beam profile was slightly elliptical with a M^2 of 1.3. The Rayleigh range of the focused beam at 5.6 GW peak power (pulse energy of 140 μJ) was 7.5 cm. A small portion of the laser pulse was picked off from the beam 30 cm downstream and fiber-coupled into a CCD optical spectrometer (Ocean Optics HR4000) to monitor the pulse spectrum.

There are a wide variety of materials that can be used to demonstrate the concept. We have chosen fused silica because high-optical-quality, UV grade material of different thicknesses is commercially available. The plates used in this report are 25 mm diameter round plates of 0.1, 0.2, or 0.5 mm thickness. The same plate thickness was used in every set of measurements. The first fused silica plate was placed at Brewster's angle at the waist of the beam (Fig. 1). In view of self-focusing in air, this waist position was determined empirically to be the location where the broadest transmitted spectrum is obtained. The transmitted pulse acquires nonlinear phase upon passage through the first fused silica plate and focuses to a higher intensity at a spot about 1–2 cm beyond the first plate. Now, a second plate was placed beyond this second focus. The plate's location was determined empirically to be the smallest distance

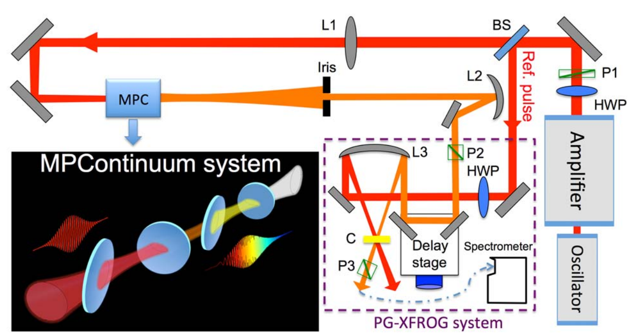

Fig. 1. Schematic of the experimental setup. BS, beam splitter; P1, thin film polarizer; P2, horizontal wire grid polarizer; P3, vertical wire grid polarizer; C, 0.15 mm thin fused silica crystal for PG-XFROG measurement; HWP, half-wave plate; L1, L2, L3, focusing elements. Insert on lower left is a sketch of the MPContinuum system, consisting of four thin fused silica plates aligned at Brewster's angle to the incident beam. HWP and P1 are used to adjust the input pulse energy. Any chirp in the pulse is compensated to provide a transform-limited pulse entering the first fused silica plate and at C. The energy of the reference pulse for PG-XFROG measurements was 20 μJ.

from the previous plate that results in the largest amount of additional spectral broadening without incurring multiple filaments and/or optical damage to the plate. The procedure of adding plates was repeated until the width of the spectrum ceased to increase. For the present input and focusing condition, this happened after the addition of a fourth plate. The final spectrum was recorded for analysis. SHG FROG was used for characterizing the input pulse. Polarization-gating cross frequency-resolved optical gating (PG-XFROG) [24] and delay-scanned spectral interferometry [25,26] were used for temporal and coherence characterization of the generated continuum.

Pulse energy measurements were taken with a thermopile (Coherent PM 10). A 60 ms integration time (averaging 60 pulses) was employed when recording each data point in all spectral-related measurements (spectral, PG-XFROG, interferometric).

3. RESULTS AND DISCUSSION

A. White Light Continuum Generation and Spectral Characterization

Most of the measurements done are at an input peak power P of 5.6 GW (pulse energy of 140 μJ). P_{cr} for fused silica is ~2 MW [14] so that P/P_{cr} in this experiment is ~2800. This input power is also well above the threshold power of 4.3 MW for filamentation in fused silica [13]. When a 0.5 mm thick fused silica was placed at the waist location, an intense white light spot appeared in the center of the beam, accompanied by many white or colored spots across the transverse profile of the beam. The transmitted pulse energy measured immediately behind the plate was about 50%. The beam diameter expanded rapidly, reaching to 3 cm at 10 cm from the position of the fused silica plate. These observations are in agreement with previous studies: when P is more than a few times larger than P_{cr}, modulational instability, multiple filamentation, multiphoton absorption and ionization, and eventually optical damage proliferate inside the material.

By shortening the optical path inside the material, the proliferation of these adverse effects could be minimized or prevented from being initiated. To test this hypothesis, we made measurements with different materials and thicknesses. The best performance to date is with 0.1 mm thin fused silica plates. Here we shall describe first the results with 0.1 mm plates. Results of other thicknesses and materials are summarized in a later section.

When the first 0.1 mm thin fused silica plate was placed at the beam waist, the transmitted pulse energy increased to 94.5% compared to the 50% of the 0.5 mm thick plate. The transmitted spectrum is slightly broadened. This spectral broadening is quite symmetric, signifying that it is mainly due to self-phase modulation (Fig. 2, orange curve). There is no degradation of the transverse mode quality. When a second 0.1 mm thin plate was placed just beyond the point where multiple filamentation and/or optical damage occur, the pulse spectrum broadened further (Fig. 2, green curve). For the present experimental conditions, the smallest spacing between the two plates before damage occurs is 3.4 cm. A blue pedestal

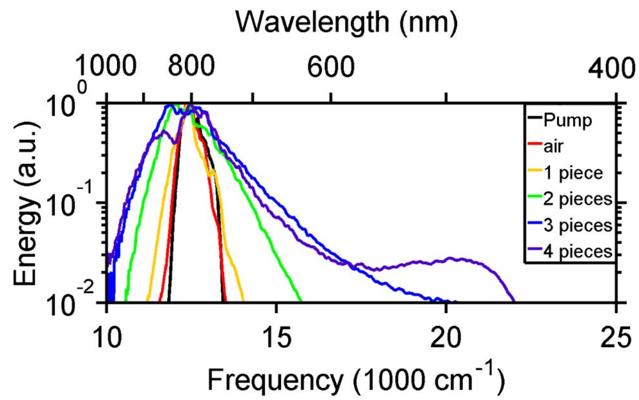

Fig. 2. Spectra recorded at a distance of 30 cm after the final fused silica plate by a Si-detector-based optical spectrometer (Ocean Optics HR4000) of the pulse after passing through air only, and after passing through different numbers of thin fused silica plates. Also shown is the spectrum of the incident pump pulse. Every spectrum has been normalized to its maximum value. The spectra show clearly rapid expansion to the blue side beginning with the second plate, and the formation of a pedestal after insertion of the fourth plate.

began to appear with the addition of a third plate and became very pronounced with a fourth plate. There was no further expansion after the fourth plate. Figure 2 shows the spectrum recorded of the input pulse and the transmitted spectrum upon the addition of each plate. The final octave-spanning spectrum extends from 450 to 980 nm at the −20 dB level. The sharp roll-off of the blue pedestal (Fig. 2, purple curve) bears a strong resemblance to SCG. This is clear indication that continuum generation in the multiple plates shares a similar mechanism with that in traditional SCG. We note that quite similar broadening can be obtained with the plates at normal incidence, but the transmitted power is reduced due to higher Fresnel reflection loss at the surfaces.

Figure 3(a) shows an original color picture of the generated pulse projected on a piece of white paper with the iris aperture wide open. It shows a white round central zone surrounded by

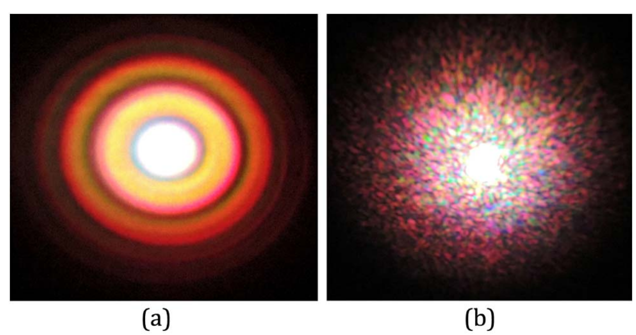

Fig. 3. (a) Original color photographic image of MPContinuum taken by a commercial portable CCD camera of 1200 megapixel resolution and exposure of 1 msec at 30 cm from the fourth plate just before the iris aperture. The central white zone is about 2 mm in diameter. (b) For comparison, we show a photograph of light generated in 0.5 mm thick fused silica pumped at the same intensity. The image in (b) was taken at 10 cm from the generating source and shows the presence of multiple filaments. The diameter of the visible portion of the image in (b) is more than 3 cm.

rings of red light. This transverse mode pattern is reminiscent of that observed at P near P_{cr} for the bulk case [10,11], but now has 100-fold higher pulse energy. For comparison, we show the picture of a pulse generated from a 0.5 mm thick fused silica showing presence of a large number of hot spots or filaments.

The measured transmitted energy after each plate was 132, 125, 114, and 109 μJ, corresponding to net transmission of 94.5%, 89.2%, 81.2%, and 77.7%, respectively. The energy loss of about 6% through each plate at Brewster's angle should primarily be caused by multiphoton absorption and ionization in fused silica. The energy within the central white zone [Fig. 3(a)] measured 30 cm from the fourth plate was 76 μJ. This corresponds to an overall conversion from the input to the white light continuum of 54%. The spectral density is estimated to range from 600 nJ/nm at 800 nm to 9.4 nJ/nm at 460 nm. This is more than two orders of magnitude higher than ever achieved in bulk material.

The measured energies exhibit excellent stability, with typical pulse energy fluctuation of ±0.83% (one standard deviation) as recorded by a power meter. Generally, the same pulse power would last through one characterization measurement described in this work, which often requires several hours of continuous operation to complete.

The spacings between the plates that resulted in the best beam quality and spectral bandwidth are 3.6, 2.1, and 1.6 cm, respectively. We find that the system is quite tolerant to the spacing between the plates. If the spacing between any pair of the plates were reduced by ~1.5 mm or more, transverse beam breakup would occur. On the other hand, if we increased the plate spacing by 15, 15, or 2 mm between plates 1 and 2, 2 and 3, and 3 and 4, respectively, the 20 dB short-wavelength roll-off point of the spectrum would reduce only by 10 nm. The spacing between plates 3 and 4 is relatively more sensitive, presumably because that is when the highly intensity-sensitive self-steepening becomes the main spectral broadening mechanism.

We isolated the white central portion of this beam from the circular rings of the transverse beam profile by an iris aperture, and then collimated it to a beam diameter of 2 mm. Hereafter, we shall name this white light portion the MPContinuum (for multiple-plates continuum).

B. Effect of Varying Input Power and Plate Thickness

We have done two series of experiments on MPContinuum generation using input pulse energy from 20 to 140 μJ to test the effect of varying the input power or energy. In the first series, we varied the incident pulse energy while keeping the pulse width and the beam waist size unchanged and recording the transmitted pulse spectrum. This has the effect of changing the incident intensity on the plates for the continuum generation. The recorded spectra are shown in Fig. 4. With the energy reduced to 120 μJ, the −20 dB bandwidth remains pretty much the same as at 140 μJ. This indicates that MPContinuum is reasonably stable to small (5%–10%) fluctuations in pulse power. Below 120 μJ, the intensity has dropped sufficiently to decrease the broadening of the spectrum.

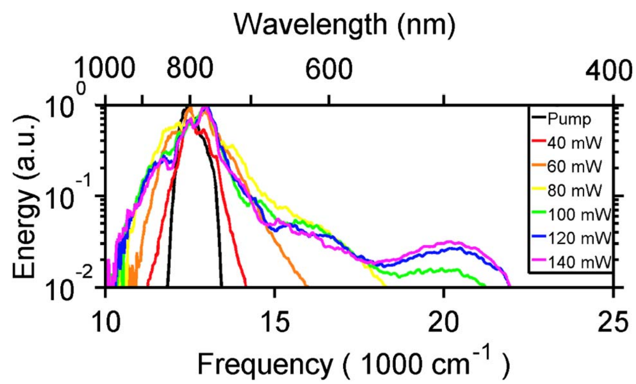

Fig. 4. MPContinuum spectrum as a function of incident pulse energy under conditions optimized for 140 μJ of incident energy. The spectrum is quite robust and is resistant to small fluctuations in pulse energy at the high end. Energies are shown as average power in mW at 1 kHz.

In the second series of experiments, the incident intensity was kept near 2×10^{13} W/cm^2 and the spectral width of the generated continuum was optimized by adjusting the spacing between the plates for each input energy. With a lower pulse energy, the corresponding Rayleigh range is shorter and the plate spacings should be less than in the 140 μJ case. This was indeed the case. For example, in the case of 40 μJ input energy, the optimal plate spacings were 1.5, 0.65, and 0.4 cm, respectively. In spite of different incident pulse energies, the spectra of all MPContinua were similar. The conversion efficiency from input to MPContinuum stayed around 50% for the entire input energy range. The beam mode also remained similar to that shown in Fig. 3(a). This large dynamic range in permissible pulse energies and peak powers highlights the flexibility and versatility of MPContinuum generation. We have not gone below 20 μJ because the Rayleigh range has become 0.4 cm and the plates were nearly touching each other. Similarly, we were limited by available optics and cannot go to higher pulse energy while keeping the intensity within the safe range.

We did measurements for 0.2 mm thin plates. There is also spectral broadening. However, the roll-off on the blue edge occurred at a longer wavelength of about 500 nm. The spectrum is not as broad as with the 0.1 mm thin plates. Plates thinner than 0.1 mm are not readily available. We are attempting to get custom-polished thinner plates to test if further broadening can be achieved. Mixing the thickness of plates has not been tried, but it will be an interesting variable that is available when optimizing the performance of MPContinuum in the future.

C. Spatial, Temporal, and Phase Coherence

Quantitative spatial characterization was done with a CCD beam profiler (Fig. 5). In order to arrive at this beam mode, it was necessary to adjust the spacing (~1–2 mm) between the first and the second plates along the propagation direction followed by a slight adjustment of less than 1 mm on the location of the fourth plate. The locations of the second and third plates remain unchanged. The mode quality after this adjustment yielded a M^2 of 1.21 in one axis and 1.26 in the orthogonal

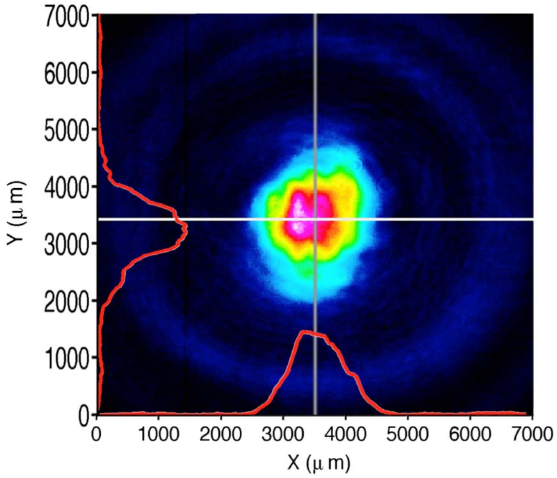

Fig. 5. False color beam profile of the MPContinuum pulse adjusted for best M^2 at 30 cm beyond the iris aperture. The red curves display the x and y transverse profile of the beam.

axis for the MPContinuum. It is not clear why the spatial mode quality is more sensitive to the longitudinal spacing between plates than spectral broadening. One possible explanation is that the transverse mode of the input pulse is slightly elliptical and is not a perfect Gaussian. The input pulse has a M^2 of 1.3.

For field characterization, we used PG-XFROG because it accepts the largest bandwidth among the family of FROG techniques [24]. The gate pulse for this measurement is a transform-limited 25 fs, 20 μJ 800 nm pulse split off from the incident pulse. Figure 6 shows the PG-XFROG results. The measurements show that the MPContinuum is chirped, spreading over 300 fs at the 10% intensity level. It is worth noting that the spectral phase is mostly quadratic and the phase noise is not very significant, so that the spectral phase may be compensated for the pulse to approach transform limit in the time domain. The present FROG result is the average of many pulses. We are mindful that local phase fluctuation from pulse to pulse may have been glossed over [27]. Single-shot measurements are being incorporated in order to improve the accuracy of the characterization [28].

We implemented the interferometric technique to check the severity of phase fluctuations caused by the complex generation process. We follow [25] and used a slightly misaligned Michelson interferometer to create Young interference fringes by spatially overlapping two MPContinua independently generated from separate but phase-locked pulses. We recorded spectrally resolved interferograms in original color with a camera, as shown in Fig. 7(a), and as white-light interference fringes [insert in Fig. 7(b)] when the two pulses were overlapping to within 1/15 fs in time. The interference fringes have good contrast and were stable for hours. The fringe visibility defined as $(I_{\max} - I_{\min})/(I_{\max} + I_{\min})$ in the white-light image is 66%, showing good phase correlation and coherence stability between the two MPContinua.

This stable phase correlation is further checked using delay-scanned spectral interferometry by scanning the time delay between the two MPContinua. The fringes in the resulting interferogram [Fig. 8(a)] are once again stable and well-resolved with good contrast. Phase coherence is preserved from pulse to pulse. The π phase shifts that appear near 750 and 825 nm are believed to be from the inherent quadrature phase shift of self-phase-modulated light interfering with residual pump radiation. The more complex interference patterns in the blue pedestal region probably arise from highly intensity-sensitive self-steepening during SCG. The appearance and the relative sharpness of the interferogram are encouraging signs

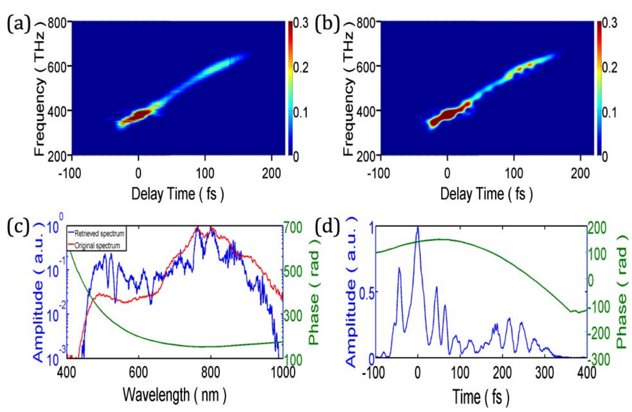

Fig. 6. PG-XFROG measurement of MPContinuum. (a) FROG trace taken by recording the spectrum transmitted through P3 in Fig. 1 at time-delay interval of 0.66 fs. Zero delay time in the horizontal axis is set as the time when the recorded peak signal is at the maximum. (b) Retrieved FROG trace with a retrieval error of 0.93%. Color codes in (a) and (b) are in log scale. (c) Retrieved spectral intensity (blue) and phase (green). The original spectrum recorded directly by the spectrometer is shown in red. All intensities are normalized to its maximum value. (d) Normalized temporal intensity (blue) and phase (green) of the MPContinuum pulse.

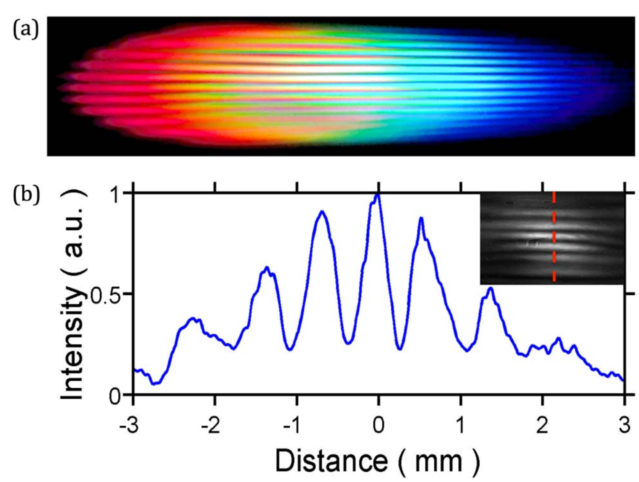

Fig. 7. Young interference fringes obtained by heterodyning at zero time delay two MPContinua independently generated from spatially separate but phase-locked pulses. (a) Spectrally resolved real color interferogram created by dispersing the white Young interference fringes with a fused silica prism. Fringes of good contrast are present at every wavelength segment. (b) Spectral-integrated intensity pattern obtained by plotting the intensity of the unresolved fringe pattern along the red dotted line shown in the inset in (b).

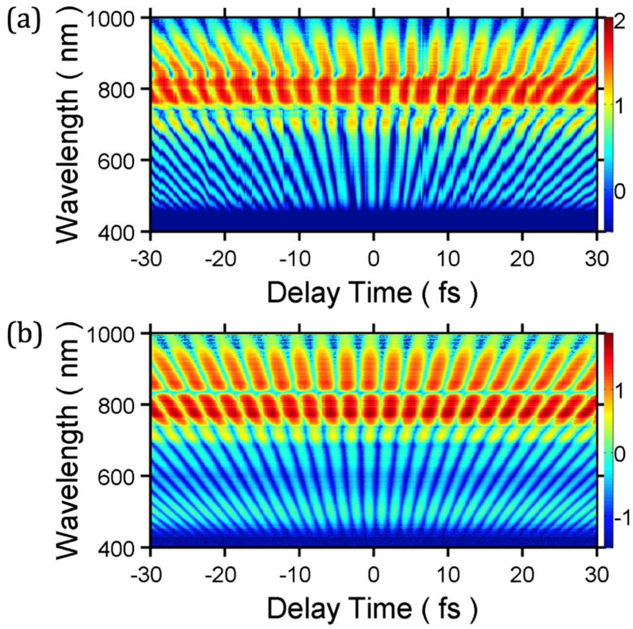

Fig. 8. (a) Time-delay spectral interferogram of MPContinuum generated by two separate but phase-locked pulses. Zero delay is when the two MPContinua are perfectly overlapping in time. The fringes show the spectrally resolved phase difference of the two MPContinua at different time delays between the two pulses. Good contrast implies reproducible spectral phase of the pulses. (b) Time-delay fringes produced by a single MPContinuum in a Michelson interferometer arrangement. The clean and sharp fringes in (b) are testimony of the high degree of stability of the interferometer used in both (a) and (b) to obtain the interferograms. Color code is in log scale.

that the MPContinuum can be compressed to a much shorter pulse by proper chirp compensation.

D. Other Materials

MPContinuum generation is not confined to fused silica. We have used other materials including BK7 glass, CaF_2, and sapphire plates. The plate thicknesses were 0.15 mm for BK7 glass and 0.2 mm for CaF_2 and sapphire. The spectral broadening we measured in these cases is comparable to the case of 0.2 mm thin fused silica and is less than that obtained with 0.1 mm thin fused silica. With sufficiently thin plates, we believe blue side extension to wavelength less than 400 nm could be achieved, especially with large bandgap materials such as the fluoride crystals [13].

4. CONCLUSION

In summary, we have demonstrated a technique of using multiple plates of a bulk material to generate an ultra-intense femtosecond white-light continuum spanning more than one octave from 450 to 980 nm. The pulse energy of the MPContinuum exceeds 76 μJ per pulse, with more than a hundredfold increase in spectral density over existing bulk sources. It has a respectable mode quality of $M^2 = 1.25$. The MPContinuum is robust, has good energy stability, and exhibits excellent spectral and temporal phase coherence to suggest that the pulse is compressible to a nearly transform-limited pulse.

MPContinuum generation possesses the merits of SCG in gases which have high pulse energy and good spatial mode quality, and it preserves the advantages of a solid medium of being compact, simple, stable, and highly reproducible. The generation scheme is extremely flexible and versatile, suitable for a wide range of input power and material. With these attributes, MPContinuum is promising in enhancing many existing applications and in enabling new applications in ultrafast science and extreme nonlinear optics. A few examples of these likely applications include high-energy seed in ultrabroadband chirped pulse amplification, isolated-pulse high harmonic generation with very high rep rate lasers, large area optical coherence tomography, and saturation microscopy and metrology with improved precision.

FUNDING INFORMATION

Ministry of Education, Taiwan (Aim for the Top University Program); Ministry of Science and Technology, Taiwan (101-2112-M-001-008-, 102-2112-M-001-010-, 103-2221-E-007-056).

ACKNOWLEDGMENT

We thank Günter Steinmeyer and Rick Trebino for many helpful discussions.

REFERENCES

1. R. R. Alfano, ed., *The Supercontinuum Laser Source* (Springer-Verlag, 1989).
2. C. P. Hauri, W. Kornelis, F. W. Helbing, A. Heinrich, A. Couairon, A. Mysyrowicz, J. Biegert, and U. Keller, "Generation of intense, carrier-envelope phase-locked few-cycle laser pulses through filamentation," Appl. Phys. B **79**, 673–677 (2004).
3. A. Wirth, M. Th. Hassan, I. Grguraš, J. Gagnon, A. Moulet, T. T. Luu, S. Pabst, R. Santra, Z. A. Alahmed, A. M. Azzeer, V. S. Yakovlev, V. Pervak, F. Krausz, and E. Goulielmakis, "Synthesized light transients," Science **334**, 195–200 (2011).
4. T. Brabec and F. Krausz, "Intense few-cycle laser fields: frontiers of nonlinear optics," Rev. Mod. Phys. **72**, 545–591 (2000).
5. D. J. Jones, S. A. Diddams, J. K. Ranka, A. Stentz, R. S. Windeler, J. L. Hall, and S. T. Cundiff, "Carrier-envelope phase control of femtosecond mode-locked lasers and direct optical frequency synthesis," Science **288**, 635–639 (2000).
6. A. Apolonski, A. Poppe, G. Tempea, Ch. Spielmann, Th. Udem, R. Holzwarth, T. W. Hänsch, and F. Krausz, "Controlling the phase evolution of few-cycle light pulses," Phys. Rev. Lett. **85**, 740–743 (2000).
7. T. Udem, R. Holzwarth, and T. W. Hansch, "Optical frequency metrology," Nature **416**, 233–237 (2002).
8. D. Wildanger, E. Rittweger, L. Kastrup, and S. W. Hell, "STED microscopy with a supercontinuum laser source," Opt. Express **16**, 9614–9621 (2008).
9. G. Humbert, W. Wadsworth, S. Leon-Saval, J. Knight, T. Birks, P. St. J. Russell, M. Lederer, D. Kopf, K. Wiesauer, E. Breuer, and D. Stifter, "Supercontinuum generation system for optical coherence tomography based on tapered photonic crystal fibre," Opt. Express **14**, 1596–1603 (2006).
10. A. L. Gaeta, "Catastrophic collapse of ultrashort pulses," Phys. Rev. Lett. **84**, 3582–3585 (2000).
11. A. Couairon and A. Mysyrowicz, "Femtosecond filamentation in transparent media," Phys. Rep. **441**, 47–189 (2007).
12. S. L. Chin, *Femtosecond Laser Filamentation*, Vol. **55** of Springer Series on Atomic, Optical, and Plasma Physics (Springer, 2010).

13. A. Brodeur and S. L. Chin, “Band-gap dependence of the ultrafast white-light continuum,” Phys. Rev. Lett. **80**, 4406–4409 (1998).
14. W. Liu, S. Petit, A. Becker, N. Aközbek, C. M. Bowden, and S. L. Chin, “Intensity clamping of a femtosecond laser pulse in condensed matter,” Opt. Commun. **202**, 189–197 (2002).
15. L. Sudrie, A. Couairon, M. Franco, B. Lamouroux, B. Prade, S. Tzortzakis, and A. Mysyrowicz, “Femtosecond laser-induced damage and filamentary propagation in fused silica,” Phys. Rev. Lett. **89**, 186601 (2002).
16. A. Couairon, L. Sudrie, M. Franco, B. Prade, and A. Mysyrowicz, “Filamentation and damage in fused silica induced by tightly focused femtosecond laser pulses,” Phys. Rev. B **71**, 125435 (2005).
17. N. T. Nguyen, A. Saliminia, W. Liu, S. L. Chin, and R. Vallée, “Optical breakdown versus filamentation in fused silica by use of femtosecond infrared laser pulses,” Opt. Lett. **28**, 1591–1593 (2003).
18. F. Silva, D. R. Austin, A. Thai, M. Baudisch, M. Hemmer, D. Faccio, A. Couairon, and J. Biegert, “Multi-octave supercontinuum generation from mid-infrared filamentation in a bulk crystal,” Nat. Commun. **3**, 807 (2012).
19. M. Kretschmar, C. Brée, T. Nagy, A. Demircan, H. G. Kurz, U. Morgner, and M. Kovacev, “Direct observation of pulse dynamics and self-compression along a femtosecond filament,” Opt. Express **22**, 22905–22916 (2014).
20. L. Bergé, S. Skupin, and G. Steinmeyer, “Temporal self-restoration of compressed optical filaments,” Phys. Rev. Lett. **101**, 213901 (2008).
21. S. Bohman, A. Suda, T. Kanai, S. Yamaguchi, and K. Midorikawa, “Generation of 5.0 fs, 5.0 mJ pulses at 1 kHz using hollow-fiber pulse compression,” Opt. Lett. **35**, 1887–1889 (2010).
22. M. Li, S. Menon, J. P. Nibarger, and G. N. Gibson, “Ultrafast electron dynamics in femtosecond optical breakdown of dielectrics,” Phys. Rev. Lett. **82**, 2394–2397 (1999).
23. A. Q. Wu, I. H. Chowdhury, and X. Xu, “Femtosecond laser absorption in fused silica: numerical and experimental investigation,” Phys. Rev. B **72**, 085128 (2005).
24. R. Trebino, *Frequency-Resolved Optical Gating: The Measurement of Ultrashort Laser Pulses* (Kluwer, 2002).
25. M. Bellini and T. W. Hansch, “Phase-locked white-light continuum pulses: toward a universal optical frequency-comb synthesizer,” Opt. Lett. **25**, 1049–1051 (2000).
26. X. Gu, M. Kimmel, A. Shreenath, R. Trebino, J. Dudley, S. Coen, and R. Windeler, “Experimental studies of the coherence of microstructure-fiber supercontinuum,” Opt. Express **11**, 2697–2703 (2003).
27. M. Rhodes, G. Steinmeyer, J. Ratner, and R. Trebino, “Pulse-shape instabilities and their measurement,” Laser Photon. Rev. **7**, 557–565 (2013).
28. T. C. Wong, M. Rhodes, and R. Trebino, “Single-shot measurement of the complete temporal intensity and phase of supercontinuum,” Optica **1**, 119–125 (2014).